Ballistic deposition patterns beneath a growing Kardar-Parisi-Zhang interface

Konstantin Khanin,[1] Sergei Nechaev,[2,3,4] Gleb Oshanin,[5,4] Andrei Sobolevski,[6,4] and Oleg Vasilyev[7,8]
[1]*Department of Mathematics, University of Toronto, 100 St. George Street, Toronto, Ontario, Canada, M5S 3G3*
[2]*LPTMS, Université Paris Sud, 91405 Orsay Cedex, France*
[3]*P. N. Lebedev Physical Institute of the Russian Academy of Sciences, 53 Leninski Avenue, 119991 Moscow, Russia*
[4]*J.-V. Poncelet Laboratory, Independent University of Moscow, 11 B. Vlasievski per., 119002 Moscow, Russia*
[5]*LPTMC, Université Paris 6, 4 Place Jussieu, 75252 Paris, France*
[6]*A. A. Kharkevich Institute for Information Transmission Problems of the Russian Academy of Sciences, 19 B. Karetny per., 127994 Moscow, Russia*
[7]*Max-Planck-Institut für Metallforschung, Heisenbergstr. 3, D-70569 Stuttgart, Germany*
[8]*Institut für Theoretische und Angewandte Physik, Universität Stuttgart, Pfaffenwaldring 57, D-70569 Stuttgart, Germany*
(Received 25 June 2010; published 6 December 2010)

We consider a (1+1)-dimensional ballistic deposition process with next-nearest-neighbor interactions, which belongs to the Kardar-Parisi-Zhang (KPZ) universality class. The focus of our analysis is on the properties of structures appearing in the bulk of a growing aggregate: a forest of independent clusters separated by "crevices." Competition for growth (mutual screening) between different clusters results in "thinning" of this forest, i.e., the number density $c(h)$ of clusters decreases with the height h of the pattern. For the discrete stochastic equation describing the process we introduce a variational formulation similar to that used for the randomly forced continuous Burgers equation. This allows us to identify the "clusters" and crevices with minimizers and shocks in the Burgers turbulence. Capitalizing on the ideas developed for the latter process, we find that $c(h) \sim h^{-\alpha}$ with $\alpha = 2/3$. We compute also scaling laws that characterize the ballistic deposition patterns in the bulk: the law of transversal fluctuations of cluster boundaries and the size distribution of clusters. It turns out that the intercluster interface is superdiffusive: the corresponding exponent is twice as large as the KPZ exponent for the surface of the aggregate. Finally we introduce a probabilistic concept of ballistic growth, dubbed the "hairy" Airy process in view of its distinctive geometric features. Its statistical properties are analyzed numerically.

DOI: 10.1103/PhysRevE.82.061107 PACS number(s): 02.50.−r, 05.10.−a, 05.40.−a

I. INTRODUCTION

Growth of aggregates by stochastic deposition of elementary units was extensively studied over the past few decades [1]. Much effort has been put into theoretical, numerical, and experimental investigation of the resulting patterns. Several theoretical models have been proposed, including the famous Kardar-Parisi-Zhang (KPZ) [2] and Edwards-Wilkinson [3] models, the restricted solid-on-solid [4] and Eden [5] models, the models of molecular-beam epitaxy [6], polynuclear growth (PNG) [7–11], and several ramifications of the ballistic deposition (BD) model [12–15]. Within the latter model, in the simplest setting, one assumes that elementary units ("particles") follow ballistic trajectories in space and adhere sequentially to a growing aggregate. Despite its extremely transparent geometric formulation, the problem of stochastic growth in the BD model remains one of the most challenging subjects in statistical mechanics.

The available theoretical analysis of stochastic deposition focuses almost exclusively on the properties of the enveloping surface $h(x,t)$. Here we quote just a few prominent results. The scaling relations characterizing the surface of a growing aggregate are

$$\langle \mathrm{Var}\, \tilde{h}(x,t)\rangle^{1/2} \sim t^{1/3},$$

$$\langle \tilde{h}(x,t)\tilde{h}(x+t^{2/3}l,t)\rangle - \langle \tilde{h}\rangle^2 \sim t^{2/3}F(l),$$

where $\tilde{h}(x,t)=h(x,t)-vt$ is the "detrended" profile of the surface [$v=\lim_{t\to\infty} t^{-1}h(x,t)$ being the average growth rate of the aggregate], $F(l)$ is a rescaled correlation function, and the angle brackets here and below denote averaging with respect to different realizations of the process. The exponents 1/3 and 2/3 were determined already in Ref. [2] for the original KPZ model and then observed in a variety of other growth models. In Refs. [8,16] it was first realized that the distribution of a rescaled PNG surface height $t^{-1/3}[h(0,t)-2t]$ converges as $t\to\infty$ to the Tracy-Widom distribution [17] for the Gaussian unitary ensemble, which appears in the theory of random matrices. Moreover, the full rescaled PNG surface $t^{-1/3}[h(xt^{2/3},t)-2t]+x^2$ converges to a version of the Airy stochastic process $\mathrm{Airy}_2(x)$ [9] whose one-point distributions are precisely Tracy-Widom [18]. The distribution of maximal heights of the (1+1) dimensional Edwards-Wilkinson and KPZ interfaces has been determined exactly in Ref. [19] (the distribution of the local maxima of the surface in the BD model has been calculated in Ref. [20]).

Since a similar convergence to Airy processes is observed in other dynamical models such as, e.g., the totally asymmetric simple exclusion process (TASEP) [21], it is customary to speak of the "KPZ universality class" whenever such limit behavior is present. In particular, the KPZ scaling has been shown in Refs. [22–24] to hold for the BD model in the thermodynamic limit [25].

Much less is known, however, about the structure of BD patterns *beneath* the enveloping surface. As revealed in numerical simulations, an aggregate consists of a "forest" of treelike clusters of different sizes, which are separated by a dual network of treelike channels or crevices (Fig. 1). Note,

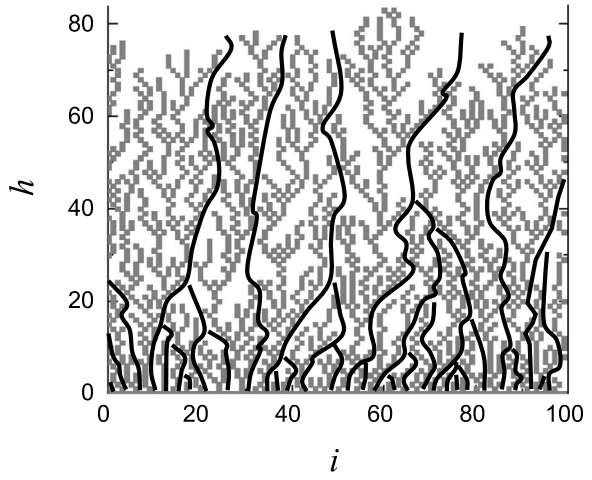

FIG. 1. Snapshot of an aggregate obtained within the ballistic deposition of $N=2000$ particles in a periodic box of size $L=100$ with next-nearest-neighbor interactions. Black lines trace the channels (crevices) between adjacent clusters.

as well, that essentially the same patterns have been observed in recent experimental analysis of electrochemically formed silver [26], a process resembling in basic features the BD model.

During the growth process, some clusters randomly collect more particles, spread more and thus isolate their neighbors from the rainfall of incident particles, suffocating their growth. Consequently, the number of clusters present at height h in a growing aggregate is a decreasing function of h. We remark that this "suffocation" mechanism, as well as the patterns emerging in the BD model, bear a certain similarity to those observed in diffusion-limited deposition of a hard-core lattice gas on a zero-temperature boundary [27], although these two models belong to different universality classes and thus their quantitative behaviors are different.

In the present work we study the bulk properties of aggregates formed in the BD process. Our analysis is based on a systematic analogy with turbulent structures in randomly forced Hamilton-Jacobi equations [28,29]. This allows us to conclude that BD belongs to a large group of models within the KPZ universality class, such as the PNG model, a totally asymmetric simple exclusion process, and others. We consider it as an important conceptual result of our work because it puts the BD model under study into a wider context. Further on, we show that the BD model, like other above mentioned models, admits a variational formulation. Capitalizing on the ideas developed in Refs. [28,29], we define analytically the decay of the number density $c(h)$ of clusters at height h, $c(h)\sim h^{-\alpha}$ with $\alpha=2/3$. We show that the horizontal mean-square displacement $\langle \Delta x^2(h)\rangle$ of a cluster's boundary at height h follows $\langle \Delta x^2(h)\rangle \sim h^{\beta}$ with $\beta=4/3$, and we also show that the "mass" m distribution $P(m)$ of clusters decays as $P(m)\sim m^{-7/5}$. Note that the high value of β, which is twice as large as the KPZ exponent, implies the superdiffusive behavior of the intercluster interface.

These findings are well supported by our numerical simulations shown below. Note, as well, that these results agree very well with those found in the experimental analysis of electrodeposition of silver [26].

Finally, the analogy with the Hamilton-Jacobi dynamics enables us to suggest a concept of a hairy Airy process, an extension of classical Airy processes which also takes into account the geometrical structure of the optimal paths (maximizers of the action, see Sec. III). The random field of optimal paths arises naturally in the context of stochastically forced Burgers equation [28,29].

The paper is organized as follows. In Sec. II we formulate the model, define its main structural features and introduce basic notations. Section III contains an analysis of the structural similarity of BD patterns to "minimizers" and "shocks" in the Burgers turbulence [29], based on the common variational formulation of the two models. Building on these developments, in Sec. IV we compute several scaling exponents characterizing the bulk structure of the aggregates formed during ballistic deposition. Next, in Sec. V we discuss the KPZ scaling in the BD model and introduce the notion of a hairy Airy process. Section VI contains concluding remarks.

II. MODEL AND BASIC DEFINITIONS

A. NNN ballistic deposition model

A standard $(1+1)$-dimensional BD model with next-nearest-neighbor (NNN) interactions can be formulated as follows (see also Refs. [22–24]). Consider a box divided into L columns of unit width each, enumerated with index $i(i=1,2,\ldots,L)$. For simplicity we assume the periodic boundary conditions so that the leftmost and the rightmost columns are neighbors, and identify the index value 0 with L.

At the initial time $t=0$ the system is empty. Then, at each time step $t=1,2,\ldots,t_{\max}$, an elementary unit (particle) of height ℓ and width 1 is deposited at a column $i(t)$ chosen randomly with uniform distribution. Define

$$\eta(i,t)=\begin{cases}1, & i=i(t)\\ 0, & i\neq i(t).\end{cases} \tag{1a}$$

As shown in Fig. 1, particles deposited in adjacent columns interact in such a way that they can only touch each other at corners or at top and bottom, but never along their vertical sides. Let the height of column i at time $t-1$ be $h(i,t-1)$. Upon adding a particle it changes according to

$$h(i,t)=\begin{cases}\max\{h(i-1,t-1),h(i,t-1),h(i+1,t-1)\}+\ell, & \eta(i,t)=1\\ h(i,t-1), & \eta(i,t)=0.\end{cases} \tag{1b}$$

This dynamics is supplemented with the initial condition $h(i,0)\equiv 0$ for all $1\le i\le L$. Equations (1a) and (1b) completely describe updating rules for the NNN discrete ballistic deposition.

We will use Eq. (1b) represented in a different form. Define the "thin" and "thick" discrete "δ functions"

$$L^0(k,i)=\begin{cases}\infty & |k-i|>0\\ 0 & |k-i|=0,\end{cases}\qquad L^1(k,i)=\begin{cases}\infty & |k-i|>1\\ 0 & |k-i|\le 1.\end{cases} \tag{2}$$

Consider first the trivial dynamics described by the equation $h(i,t)=h(i,t-1)$. It can be rewritten as $h(i,t)=\max_k[h(k,t-1)-L^0(k,i)]$: indeed, $\max_{k\neq i}[h(k,t-1)-\infty]\equiv-\infty$ and therefore $h(i,t)=\max\{h(i,t-1),-\infty\}=h(i,t-1)$. It is now clear that the stochastic Eq. (1b) can be recast in the form

$$h(i,t)=\max_k[h(k,t-1)-L^{\eta(i,t)}(k,i)]+\ell\,\eta(i,t). \tag{3}$$

This dynamics should be compared with the commonly used discrete equation with "additive noise" describing the evolution of an interface $h'(i,t)$ in a $(1+1)$-dimensional polynuclear growth [9], which in our notation takes the form

$$h'(i,t)=\max_k[h'(k,t-1)-L^1(k,i)]+\ell\,\eta(i,t). \tag{4}$$

According to Eq. (3), the height $h(i,t)$ remains unchanged if nothing is deposited to column i at time t. On the contrary, in Eq. (4) the height $h'(i,t)$ relaxes spontaneously even in the absence of deposition to column i at time t because $h'(i,t)$ is defined to be the maximum of the triple $\{h'(i-1,t-1),h'(i,t-1),h'(i+1,t-1)\}$. Note that process described by Eq. (3) is sometimes referred to as "dynamics with multiplicative noise."

B. Clusters, crevices, and scaling exponents of a growing aggregate

Let us now take a closer look at Fig. 1. We say that two particles in the aggregate are *connected* if they touch one another at corners or if one is situated directly on top of the other.

It often happens that the upper particle is connected simultaneously to two lower particles. For reasons that will become clear shortly, it is better to avoid these "one-on-two" configurations. The model is therefore slightly augmented: one assumes in Eqs. (1b) and (3) that

$$\ell=\ell(t)=1+10^{-10}\xi(t), \tag{5}$$

where $\xi(t)$ are independent normal random variables. It is clear and well supported by numerical experiments that this modification removes the possibility of one-on-two configurations while preserving, within the limits of statistical errors, statistical characteristics of the aggregate for $\ell\equiv 1$. Alternatively one might resolve one-on-two configurations for $\xi=0$ by simply disconnecting the upper particle from one of its two lower neighbors at random. In either way, elimination of one-on-two configurations allows us to define a unique "path" corresponding to every particle, namely, a backward directed chain of connected particles going from a given particle to the bottom level of the aggregate.

Consider all connected paths originating from the topmost particles. These paths can merge. We define the backbone of a cluster as the connected set of such paths, i.e., the union of all paths that end up at the same bottom level particle. It is easy to see that the bottom level particles are split into two classes: those that are reached by the paths originated at the top of the aggregate and those that are not. Obviously the first class gets smaller as t increases. For every particle from this class define cluster as the collection of all paths ending up at this particle. The difference between a backbone and a cluster is that clusters contain paths not necessarily originating from the top level particles.

We say that a pair of two top level particles occupying adjacent columns defines a shock, which is located between them, if they belong to two different clusters. The channel of white space between two neighboring clusters is called a crevice. Clearly, every crevice is associated with a shock at the top, and the connected paths from top particles defining the shock form the left and right boundary of a crevice. Connecting shocks at adjacent time moments, we get curves that branch backward in time and play a role dual to that of backbones. These curves are sketched in Fig. 1 in black.

It is clear from Fig. 1 that many channels that are initially present at bottom of the bulk then merge at some height, blocking the growth of the clusters situated in between. Thus the crevices form a treelike structure just as the clusters do, but contrary to the clusters they merge upward. This causes the number of percolating clusters and crevices in the box to decrease as a function of h. In the thermodynamic limit this behavior is characterized by the following three scaling exponents whose values are identified in Sec. IV.

The thinning exponent α characterizes the expected number density $c(h)$ of percolating crevices (or, equivalently, percolating clusters) at height h, see Fig. 2(a):

$$c(h)=\frac{1}{L}\langle N_h\rangle\sim(h/L)^{-\alpha}, \tag{6}$$

where N_h is the number of clusters surviving up to height h in a given realization of the deposition process.

The roughness exponent β characterizes the mean-square displacement (in the units of L) of the boundary of a percolating cluster between the bottom of the bulk and a specified height h, see Fig. 2(b):

$$\langle\Delta x^2(h)\rangle\sim(h/L)^{\beta}. \tag{7}$$

The mass exponent τ characterizes the mass distribution of clusters:

$$P(m)\sim m^{-\tau}, \tag{8}$$

where $P(m)$ is the fraction of clusters of mass m in the ensemble, see Fig. 2(c).

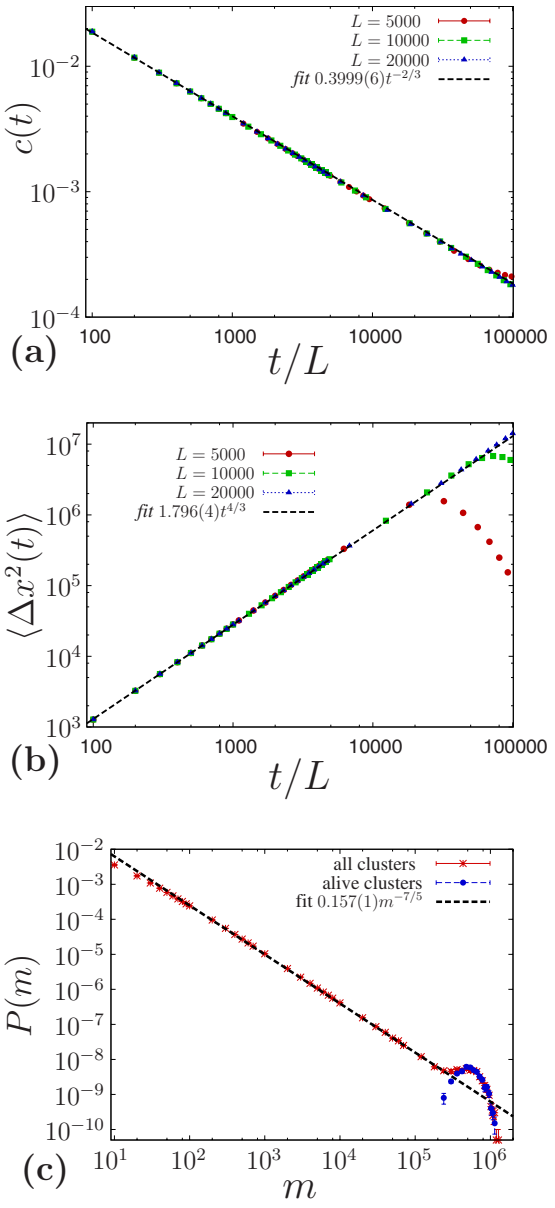

FIG. 2. (Color online) Numerical evidence for scaling exponents identified in the text. Note that the mean height $\langle h \rangle$ of the aggregate is proportional to the number of dropping events per column, $\langle h \rangle \sim t/L$. We therefore plot the quantities of interest as functions of t/L rather than h: (a) the number density of percolating clusters (and crevices) as function of t/L; (b) the mean-square displacement of the boundary of a percolating cluster $\langle \Delta x^2 \rangle$ as function of t/L; (c) the probability $P(m)$ to find in a large system a cluster of mass m. Note that departures of numerical data from theoretical predictions appear here due to evident finite-size effects.

III. BALLISTIC DEPOSITION AND BURGERS TURBULENCE

A. Variational formulation of the BD

The discrete equation

$$h(i,t) = \max_k [h(k,t-1) - L(k,i,t)] + \ell\, \eta(i,t), \tag{9}$$

whose particular cases for specific choices of $L(k,i,t) = L^{\eta(i,t)}(k,i)$ and $L(k,i,t) = L^1(k,i)$ are correspondingly the BD model Eq. (3) and the discrete PNG model Eq. (4), admits a natural variational formulation.

Fix some initial condition $h(i,0)$ and consider the discrete "variational" problem of finding a trajectory $[\gamma(0), \gamma(1), \ldots, \gamma(t)]$ that satisfies the "boundary condition" $\gamma(t) = i$ and maximizes the discrete "action"

$$\mathcal{A}_0^t(\gamma) = h[\gamma(0),0] - \sum_{1 \le s \le t} \{L[\gamma(s-1), \gamma(s), s] - \ell\, \eta[\gamma(s), s]\}. \tag{10}$$

The function in the square brackets plays a role of a discrete "Lagrangian" of the system. The problem bears an obvious resemblance to the zero-temperature limit of the free energy of a statistical system, expressed as the sum over configurations γ:

$$\lim_{T \to 0} T \ln(e^{(1/T)A_1} + \cdots + e^{(1/T)A_N}) \to \max\{A_1, \ldots, A_N\}.$$

Another obvious connection is with mechanics, where the dynamical trajectory can be found by optimizing the corresponding action (in our case, at variance with the usual convention, the action is *maximized*).

Action maximization in Eq. (10) is related to solving Eq. (9) as follows. To be specific, consider the BD growth Eq. (3), where particles are added to the system as "dropping events" $(i(s), s)$ in $(1+1)$ dimensional discrete space time. Maximization of the action $\mathcal{A}_0^t$ in Eq. (10) amounts to finding a trajectory that terminates at (i,t) and passes through a maximal number of dropping events under the following constraint: the trajectory stays constant, $\gamma(s) = \gamma(s-1)$, unless $\gamma(s-1) = i(s) \pm 1$, i.e., there is a dropping event in adjacent column. In the latter case the trajectory may (but does *not* necessarily have to) jump to $i(s)$ at time step s. Note that for the PNG model Eq. (4) this constraint is relaxed: a trajectory may jump at all times, but only to adjacent columns. Otherwise the two models are structurally similar, and the rest of the argument in this subsection applies to both.

The lack of a strict obligation to pass through an adjacent dropping event allows to "collect" dropping events more efficiently: it is easy to construct trajectories for which it is more profitable, from the point of view of maximizing the number of dropping events, to skip some isolated dropping events in order not to be driven away from a later series of several adjacent dropping events.

Direct maximization of the action Eq. (10) is a difficult problem because the solution depends on the whole future history of dropping events. Observe however that for all $1 \le j \le L$, $1 \le s \le t$ the height function $h(j,s)$ gives the maximal number of dropping events available for a trajectory coming to the point (j,s), and this fact can be exploited to construct a maximizing trajectory in *reverse* time.

Consider again the BD case where $L(k,j,s) = L^{\eta(j,s)}(k,j)$. Then the maximizing trajectory passing through an arbitrary (i,t) can be reconstructed by setting $\gamma(t) = i$ and solving recursively

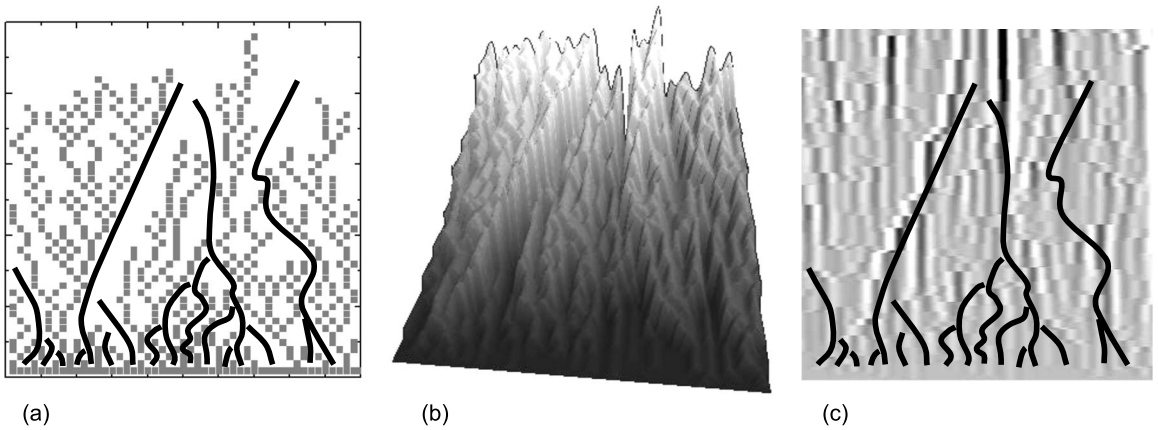

FIG. 3. (a) An aggregate growing by sequential deposition with highlighted crevices; (b) the growing aggregate in the (2+1)-dimensional space time; (c) density plot of second local difference (discrete analog of second derivative) of the height, which highlights the discontinuities corresponding to shocks. Panels (a) and (c) represent front and top views, respectively, of the three-dimensional structure in panel (b).

$$\gamma(s-1) = \arg\max_k \{h(k,s-1) - L^{\eta(\gamma(s),s)}(k,\gamma(s))\} + \ell\,\eta(\gamma(s),s) \tag{11}$$

for $s=t,t-1,\ldots,1$. Here $\arg\max_k$ is the standard notation for the value of k that provides maximum to the expression in the right hand side of Eq. (11).

The algorithmic implementation of the above goes as follows. Solve first Eq. (9) "upstairs" starting from given initial conditions and obtain the set of values $h(1,s),h(2,s),\ldots,h(L,s)$ for all $0\le s\le t$. Then choose a specific point, say (i,t), and restore the path to this point going "downstairs," i.e., back in time, by solving Eq. (11) step by step. This procedure defines a trajectory maximizing the action $\mathcal{A}_0^t$ in Eq. (10). This class of algorithms is known in the optimization theory as *dynamic programming*, and Eq. (9) is called the *Bellman equation* (see, e.g., the classical book [30]).

B. BD aggregates and the Burgers turbulence

It turns out that there is a far-reaching analogy between the BD deposition model and phenomenology of "shocks" and "minimizers" for the Burgers or Hamilton-Jacobi equation with random forcing (see, e.g., Ref. [29]). We first recall the latter.

Consider the inviscid Burgers equation

$$\partial_t u + u\partial_x u = -\partial_x \eta(x,t),$$

where $\eta(x,t)$ is the forcing potential. The substitution $u=\partial_x h$ transforms this equation into

$$\partial_t h + (\partial_x h)^2/2 + \eta(x,t) = 0.$$

More generally, one can consider the Hamilton-Jacobi equation

$$\partial_t h + H(\partial_x h) + \eta(x,t) = 0, \tag{12}$$

where $H(p)$ is a convex function representing the kinetic energy. Using the Legendre transform representation $H(p)=\max_v[pv-L(v)]$, one can write

$$\partial_t h + v\partial_x h - L(v) + \eta(x,t) \le 0$$

with equality only for $\partial_x h=L'(v)$, i.e., $v=H'(\partial_x h)$. Hence along any trajectory $\gamma(t)$ the rate of change in h is bounded by the Lagrangian

$$\frac{d}{dt}h(\gamma,t) \le L(\dot\gamma) - \eta(\gamma,t)$$

(here $\dot\gamma=d\gamma/dt$), which implies for any γ passing through x at time t that

$$h(x,t) \le \mathcal{A}_0^t[\gamma] = h[\gamma(0),0] + \int_0^t [L(\dot\gamma) - \eta(\gamma,s)]ds \tag{13}$$

with equality only for minimizers of the action, which must satisfy the equation

$$\dot\gamma(t) \equiv H'[\partial_x h(\gamma,t)]. \tag{14}$$

The Hamilton-Jacobi Eq. (12) is thus intimately connected with the variational problem of minimizing the action Eq. (13), just as the Bellman Eq. (9) arises in maximization of the discrete "action" Eq. (10). Note in particular the similar structure of the action (the difference in sign results in maximization replacing minimization in the discrete case). Moreover, a known solution h to Eq. (12) allows us to reconstruct minimizing trajectories using Eq. (14), much as Eq. (11) generates maximizing trajectories in the discrete problem.

It is therefore natural to consider the discrete maximizing trajectories defined in the previous subsection as analogs of continuous minimizers. There is one apparent difference: continuous minimizers never cross, while discrete maximizing paths merge and form treelike structures. However continuous minimizers have a tendency to approach each other with exponential rate in reverse time due to hyperbolicity, and in the discrete case the same hyperbolicity manifests itself in the exponentially decreasing probability for two adjacent maximizers to stay separate as time runs backward.

We are now in position to establish the relation between discrete maximizers and connected paths defined within the aggregate in Sec. II. Lift the maximizing trajectories to the (i,t,h) space by setting $h=\mathcal{A}_0^t(\gamma)$ for a maximizer γ such that $\gamma(t)=i$. Then connected paths are given by the projection of these "lifted" maximizers to the (x,h) plane (see Fig. 3). In other words, the intervals of time between successive dropping events along a maximizer are collapsed into unit steps in h. Correspondingly the transversal fluctuations of maximizers as a function of time are transformed to transversal fluctuations of connected path as a function of height h.

The analogy between continuous minimizers and discrete maximizers extends to shocks. In the Burgers turbulence it typically happens that two or more minimizing trajectories, which start at different initial locations, pass through same point x at time t so that the map from (x,t) to the initial location is discontinuous (see, e.g., [29]). These discontinuities are called shocks; in space time they form continuous shock curves. This definition is obviously parallel to the definition of shocks given in the BD setting in Sec. II (and has inspired the latter).

IV. SCALING ANALYSIS OF BD PATTERNS

A. Thinning of a forest of clusters and roughness of clusters' boundaries

Relying on the connection between shocks and boundaries of clusters, we can directly transfer the scaling arguments of statistics of shocks developed in Ref. [29] to the scaling analysis of a growing BD aggregate and determine the values of the scaling exponents α and β in the dependencies $c(h)\sim h^{-\alpha}$ and $\langle \Delta x^2(h)\rangle \sim h^{\beta}$ defined correspondingly in Eqs. (6) and (7). Recall that $c(h)$ is the averaged number density of clusters percolating to height h and $\langle \Delta x^2(h)\rangle$ is the mean-square displacement of a cluster boundary at height h.

Denote by $d(t)$ the horizontal size of a given cluster at time t. At $t=0$ the cluster has zero size, i.e., $d(0)=0$. In what follows we shall use the obvious fact that the growth time t in the sequential deposition process is proportional to the average height h of the growing aggregate and, consequently, to the cluster height [see, for example, Fig. 3(b)].

The typical value of $d(h)$ can be obtained by scaling considerations. Namely, growth of $d(h)$ is determined by two additive effects. On the one hand, there is a "driving force" promoting the "smearing" of the cluster due to the velocity fluctuations. For BD this effect can be estimated as follows. Consider clusters with size of order d. Under the uniform random rainfall of deposited particles, one cluster can randomly screen part of its neighbors, and increase its own "spot." Since different clusters are correlated weakly, it is natural to conjecture that the typical scale of fluctuations of cluster sizes is of order of $\sqrt{d}$. Thus the rate w of cluster "smearing" due to these fluctuations is $w\sim\sqrt{d}/d\sim d^{-1/2}$. Speaking more carefully, the above means that the average growth rate of the cluster of size d is

$$w=\frac{1}{d}\sum_{k\le j\le k+d}[h(j+1,t)-h(j,t)],$$

where k and $k+d$ are the left and the right boundaries of some cluster. The increments of $h(j,t)$ are uncorrelated for the uniform ballistic "rain" and $\langle h(j+1,t)-h(j,t)\rangle=0$. Hence, evidently,

$$\sum_{k\le j\le k+d}[h(j+1,t)-h(j,t)]\sim d^{1/2}, \tag{15}$$

and it is therefore natural to expect that $w\sim d^{-1/2}$, as conjectured.

On the other hand, there is a certain smearing of clusters due to a random deposition of new particles near the cluster boundary. This process can be interpreted as a "diffusion" of the boundary. Over time t this diffusion leads to the smearing of the cluster's horizontal size on typical scales of order of $\sqrt{t}$.

The typical size of a growing cluster at time t is determined by an additive contribution of these two effects:

$$d(t)\simeq wt+t^{1/2}=\frac{t}{\sqrt{d(t)}}+t^{1/2}. \tag{16}$$

For sufficiently large t, the dominant contribution to $d(t)$ comes from the first term on the right-hand side of the latter equation, which is consistent with the physical intuition. Hence, we have that

$$d(t)\sim t^{2/3}. \tag{17}$$

Since $t\sim h$, we immediately come to the conclusion that $d(h)\sim h^{2/3}$. Note that this estimate is a direct paraphrase of the arguments provided in Ref. [29] for a scaling analysis of statistics of shocks in a $(1+1)$-dimensional Burgers equation with random forcing.

The number density $c(h)$ of independent clusters surviving up to the height h is inversely proportional to the cluster size, $c(h)\sim[d(h)]^{-1}$. Hence, we find

$$c(h)\sim h^{-2/3}, \tag{18}$$

which implies that $\alpha=2/3$ [26].

Finally, a horizontal mean-square displacement $\langle \Delta x^2(h)\rangle$ of a cluster boundary at height h can be estimated straightforwardly as

$$\langle \Delta x^2(h)\rangle = d^2(h)\sim h^{4/3}, \tag{19}$$

which gives $\beta=4/3$. Note that, surprisingly, the roughness exponent describing fluctuations of the intercluster boundary is two times larger than the roughness exponent characterizing the KPZ interface. The wandering of the intercluster boundary in the BD model appears to be superdiffusive, in contrast to the diffusive evolution of the intercluster boundary observed for the diffusion limited deposition of a hard-core lattice gas on a zero-temperature boundary [27].

B. Cluster mass distribution

This subsection contains the scaling analysis of the probability $P(m)\sim m^{-\tau}$ to find a cluster of mass m in a large aggregate. To begin with, note that the number of particles, i.e., the mass $m(h)$ of a cluster percolating to height h can be obtained integrating the horizontal size, $d(h)$, of cluster at a given height:

$$m(h) \sim \int_0^h (h')^\alpha dh' \sim h^{\alpha+1}. \tag{20}$$

From Eq. (18) we know that the cumulative probability of clusters surviving until height h is of the order of $h^{-\alpha}$. This implies that the probability density of clusters at height h scales as $h^{-(\alpha+1)}dh$. In order to calculate mass distribution, we change variables from h to m, take into account that $dm \sim h^\alpha dh$, or $dh \sim h^{-\alpha}dm = m^{-\alpha/(\alpha+1)}dm$, and get

$$P(m) \sim m^{-\tau}dm \sim h^{-(\alpha+1)}dh \sim m^{-1}m^{-\alpha/(\alpha+1)}dm = m^{-(2\alpha+1)/(\alpha+1)}dm. \tag{21}$$

For $\alpha=2/3$ we get $\tau=7/5=1.4$. The exponent $\tau=7/5$ is well supported by our own numerical simulations shown in Fig. 2(c). Curiously, it also agrees quite well with the value $\tau=1.37\pm0.04$ found in experiments on cluster formation in quasi-two-dimensional electrochemically formed silver branching structures [26].

One can say that the clusters are ranked (ordered) according to their masses and m is the corresponding rank. Thus Eq. (21) has similarity with Zipf's law that appears in many areas of science ranging from word statistics in linguistics [31] to nuclear multifragmentation [32,33] where clusters have power-law distribution in sizes (masses, charges, etc.) [34].

V. FROM BD PATTERNS TO AIRY PROCESSES

A. Basics of classical KPZ scaling

Recall first the basics of classical KPZ scaling related to Airy_1 process, which is closest to our setting. The scheme described below is due to Sasamoto [21].

Consider a directed random walk on a $(1+1)$-dimensional lattice. Suppose that the space-time lattice is equipped by a random potential with independent values $\eta(i,s)$ at each point (i,s). Then for every i one can consider the maximum of an action over all random-walk paths of length t terminating at that point, i.e., define as

$$a(i,t) = \max_{\gamma:\gamma(t)=i} \sum_{1\le s\le t} \eta(\gamma(s),s),$$

where $L(k,i)$ is a kinetic part of the action that ensures a certain control of how far the trajectory γ can jump over unit time steps. It is easy to see that $t^{-1}a(i,t)\to v$ at $t\to\infty$, where v is some nonrandom constant independent of i. We now consider the rescaled process

$$A_t(x) = \frac{1}{\lambda' t^{1/3}}[a(\lambda t^{2/3}x,t) - vt]. \tag{22}$$

The main statement is that $A_t(x)$ converges as $t\to\infty$ to a universal spatially homogeneous limit process called $\mathrm{Airy}_1(x)$. Universality here means that whenever one optimizes in a disordered medium the action of a path from a point that varies over a line to a parallel line separated from the first one by distance t ("point-to-line last-passage percolation"), the process corresponding to the optimal action converges as $t\to\infty$ to the Airy_1 process.

Note that spatial homogeneity of $\mathrm{Airy}_1(x)$ immediately follows from the construction. Of course one has to ensure convergence by subtracting the mean value of order t, normalizing the difference by $t^{1/3}$ and rescaling the starting point by $t^{2/3}$. The constants λ and λ' in Eq. (22) are nonuniversal and are to be chosen properly to ensure convergence to the standard Airy process. A similarly rescaled "point-to-point" percolation results in the Airy_2 process.

B. Airy process for BD pattern

As we have shown in Sec. III the height function in the BD process can be viewed as given by maximization procedure for random paths in random potential. The only difference with the classical picture just described is related to the rarity of the deposition events. In other words, in order to achieve the displacement of order 1 in space direction one needs time of order L. This explains why time has to be rescaled.

The most natural way to do this is through a local stochastic change in time variable. Namely, we collapse the time between two deposition events to 1. This is exactly the transformation from (lifted) maximizers to connected paths presented in Sec. III. It is therefore no surprise that the Airy_1 process can be obtained from the BD height function:

$$\lim_{t\to\infty} \frac{1}{\lambda'(t/L)^{1/3}}\{h(\lambda(t/L)^{2/3}x,t) - t/L\} = \mathrm{Airy}_1(x). \tag{23}$$

This formula simply indicates that the appropriately rescaled height function in BD is the visualization of the process which converges in the thermodynamic limit to the Airy process.

C. Hairy Airy process

The Airy_1 process carries only part of the information about the system: it is oblivious to the maximizing trajectory associated to the (rescaled) point (x,t). It is therefore natural to consider the limit

$$\left(\frac{a(\lambda t^{2/3}x,t) - vt}{\lambda' t^{1/3}}, \frac{\gamma_{\lambda t^{2/3}x,t}(ts)}{\lambda' t^{2/3}}\right) \underset{[t\to\infty]}{\to} [\mathrm{Airy}_1(x), \Gamma_x(s)], \tag{24}$$

where $\gamma_{i,t}$ is the maximizing trajectory that passes through i at time t and $\Gamma_x(s)$ is a continuous path defined over $[0,1]$ such that $\Gamma_x(1)=x$. For obvious reasons we propose to call this limit the hairy Airy process.

As we previously did, in the BD setting we collapse time intervals between adjacent deposition events to unit steps and get particle paths instead of maximizing trajectories in formula (24) above. Applying transversal rescaling $\lambda(t/L)^{2/3}x$ and height rescaling $\lambda'(t/L)^{1/3}$ as in Eq. (23), we get a realization of a hairy Airy process from the rescaled BD aggregate. This process describes the joint distribution of fluctuations of the height function and transversal displacements of cluster boundaries in the spatially homogeneous BD process.

In other words, the rescaled height function for the BD model alone is a realization of the Airy_1 process, while the

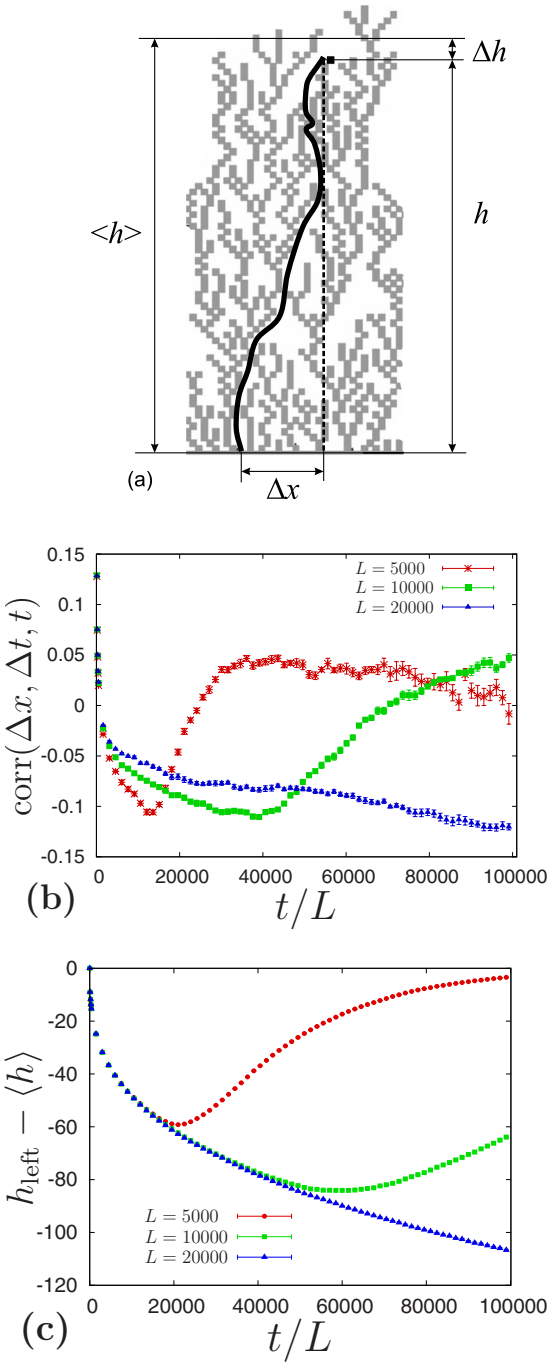

FIG. 4. (Color online) (a) Correlation between the height of cluster's boundary and the displacement of the corresponding connected path; (b) the corresponding correlation coefficient; (c) the averaged difference between the height of cluster's right boundary and the mean height of the BD growing interface.

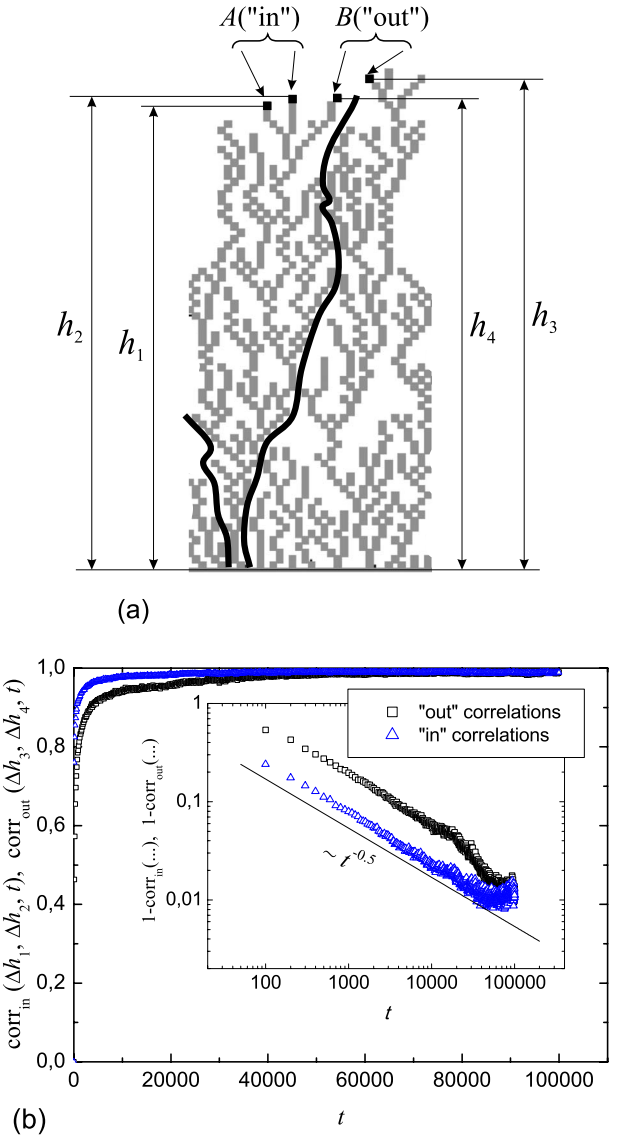

FIG. 5. (Color online) (a) Correlation between the heights inside the cluster ("in") and separated by a shock ("out"); (b) the corresponding correlation coefficients.

rescaled height function together with the rescaled forest of maximizers corresponds to a realization of the hairy Airy process. The distinctive geometric features of this joint process actually suggests the name hairy Airy process, cf. Fig. 4(a).

We demonstrate the existence of correlations in the joint distribution for the hairy Airy process by computing numerically the joint distribution of the height fluctuation Δh at the top of a shock and the corresponding displacement Δx of the cluster boundary. To be precise, we compute the correlation coefficient between the fluctuations of the displacement Δx of the right boundary of a cluster (or equivalently a backbone) and the height fluctuation Δh at the top right point of the same cluster, see Fig. 4(a). For convenience we explicitly recall here the standard definition of the correlation coefficient $\mathrm{corr}\{a,b\}$ between two random variables a and b:

$$\mathrm{corr}\{a,b\} = \frac{\langle (a-\langle a\rangle)(b-\langle b\rangle)\rangle}{\sqrt{\langle (a-\langle a\rangle)^2\rangle \langle (b-\langle b\rangle)^2\rangle}}. \tag{25}$$

Let the top right particle of some cluster be located at time t in column j. Let $h(j,t)$ be its height and $\langle h(t)\rangle$ the mean height of the whole surface at time t. Denote furthermore $h(j,t)-\langle h(t)\rangle$ by $\Delta h(j,t)$ and the displacement of the right boundary of the same cluster at time t, measured from

the position of this boundary at $t=0$, by $\Delta x_j(t)$. We fix a time t, collect for each cluster the joint information $[\Delta h(j,t),\Delta x_j(t)]$, and perform averaging over all clusters. Behavior of the corresponding time-dependent correlation coefficient $\mathrm{corr}\{\Delta h,\Delta x\}$, where the angle brackets correspond to averaging over the sample, is shown in Fig. 4(b) for different time values.

Strong correlations between the vertical and horizontal displacements of cluster boundaries are clearly seen in the data. The negative sign of these correlations is due to the fact that the height of the top right particle in a typical cluster is smaller than the averaged height of the growing BD interface. This observation is supported by Fig. 4(c), where the averaged difference between the height of the cluster right boundary and the averaged height of the interface is plotted against time. Clearly this difference is always negative and tends to zero from below as $t\to\infty$. One may speculate that growth of the leftmost- and rightmost-connected paths in a cluster is slower due to screening between neighboring clusters.

In order to better understand the influence of clusters on the morphological structure of the growing BD surface, we also compute the joint distribution of height fluctuations in two columns separated by distance $\delta=3$ in lattice units, as shown in Fig. 5(a). Two different situations are distinguished: (i) two test column belong to the same cluster (configuration A) and (ii) two test columns belong to different clusters, i.e., are separated by a shock (configuration B).

Computing the correlation coefficient $\mathrm{corr}\{\Delta h(k,t),\Delta h(m,t)\}$ according to Eq. (25), we see that correlations between $\Delta h(1,t)$ and $\Delta h(2,t)$ inside a cluster are stronger than those across a shock between different clusters.

VI. CONCLUSION

In this paper we analyzed the internal structure of an aggregate formed in a closed box in the course of a standard homogeneous ballistic deposition process with next-nearest-neighboring (NNN) interactions. Our numerical simulations showed that such an aggregate is a collection of independent clusters separated by crevices. Moreover, we realized that as the aggregate grows, the clusters compete for the incoming particles and mutually screen each other, which results in thinning of the forest of clusters; the number density $c(h)$ of clusters decreases with the height h of the pattern.

Further on, we have demonstrated that the discrete stochastic equation describing the BD process can be naturally represented in terms of a dynamic programming language associated with the so-called Bellman equation. This dynamic programming point of view allowed for a systematic translation of the study of clusters and crevices evolution in the NNN BD model into the language of maximizers and shocks in discrete equations of the Burgers or Hamilton-Jacobi type. This is the key point of our work which not only puts the model under study in a wider context but also allowed us to take an advantage of the ideas developed for the latter process. Specifically, we have found the exponents characterizing the decay of the number density of clusters, wandering of the intercluster interface and also have defined the tail of the cluster mass distribution. Our analytical results have been confirmed by extensive numerical simulations.

Finally, we introduced a kind of the Airy process characterizing ballistic deposition patterns, whose realizations define a rescaled height function together with a rescaled forest of maximizers. This very distinctive geometric feature of the process suggests the name of hairy Airy process. Statistical properties of this process were analyzed numerically.

ACKNOWLEDGMENTS

We are grateful to G. Carlier for drawing our attention to the fact that both the NNN BD model and PNG evolution processes can be expressed in terms of a Bellman equation. K.K. and A.S. are partially supported by the joint CNRS-RFBR Project No. 07-01-92217; the latter author also acknowledges the support of the French Agence Nationale de la Recherche via project BLAN 07-01-0235 OTARIE. G.O. is partially supported by Agence Nationale de la Recherche under grant Dynamique et Optimisation des Processus de Transport Intermittents (DYOPTRI).

[1] T. Halpin-Healy and Y.-C. Zhang, Phys. Rep. **254**, 215 (1995).
[2] M. Kardar, G. Parisi, and Y.-C. Zhang, Phys. Rev. Lett. **56**, 889 (1986).
[3] S. F. Edwards and D. R. Wilkinson, Proc. R. Soc. London, Ser. A **381**, 17 (1982).
[4] J. M. Kim and J. M. Kosterlitz, Phys. Rev. Lett. **62**, 2289 (1989).
[5] F. Family and T. Vicsek, J. Phys. A **18**, L75 (1985).
[6] M. A. Herman and H. Sitter, *Molecular Beam Epitaxy: Fundamentals and Current* (Springer, Berlin, 1996).
[7] P. Meakin, *Fractals, Scaling, and Growth Far From Equilibrium* (Cambridge University Press, Cambridge, 1998).
[8] M. Prähofer and H. Spohn, Phys. Rev. Lett. **84**, 4882 (2000).
[9] M. Prähofer and H. Spohn, J. Stat. Phys. **108**, 1071 (2002).
[10] J. Baik and E. M. Rains, J. Stat. Phys. **100**, 523 (2000).
[11] K. Johansson, Commun. Math. Phys. **242**, 277 (2003).
[12] B. B. Mandelbrot, *The Fractal Geometry of Nature* (Freeman, New York, 1982).
[13] P. Meakin, P. Ramanlal, L. M. Sander, and R. C. Ball, Phys. Rev. A **34**, 5091 (1986).
[14] J. Krug and P. Meakin, Phys. Rev. A **40**, 2064 (1989).
[15] D. Blömker, S. Maier-Paape, and T. Wanner, Interfaces Free Boundaries **3**, 465 (2001).
[16] J. Baik, P. Deift, and K. Johansson, J. Am. Math. Soc. **12**, 1119 (1999).
[17] C. A. Tracy and H. Widom, Commun. Math. Phys. **159**, 151 (1994).
[18] It should be noted that the BD model considered here involves the point-to-line last-passage percolation while the PNG model corresponds to the point-to-point setting [11]. Correspondingly

the limit processes are different: it is Airy_1 for the point-to-line and Airy_2 for the point-to-point. Note also that the one-point distribution for the Airy_1 process is given by the Gaussian Orthogonal Ensemble distribution rather than the Gaussian Unitary Ensemble distribution, which corresponds to Airy_2.

[19] S. N. Majumdar and A. Comtet, Phys. Rev. Lett. **92**, 225501 (2004).

[20] F. Hivert, S. Nechaev, G. Oshanin, and O. Vasilyev, J. Stat. Phys. **126**, 243 (2007).

[21] T. Sasamoto, J. Phys. A **38**, L549 (2005).

[22] G. Costanza, Phys. Rev. E **55**, 6501 (1997).

[23] F. D. A. Aarão Reis, Phys. Rev. E **63**, 056116 (2001).

[24] E. Katzav and M. Schwartz, Phys. Rev. E **70**, 061608 (2004).

[25] A. M. Vershik, S. K. Nechaev, and R. Bikbov, Commun. Math. Phys. **212**, 469 (2000).

[26] C. M. Horowitz, M. A. Pasquale, E. V. Albano, and A. J. Arvia, Phys. Rev. B **70**, 033406 (2004).

[27] S. F. Burlatsky, G. Oshanin, and M. Elyashevich, Phys. Lett. A **151**, 538 (1990).

[28] W. E, K. Khanin, A. Mazel, and Ya. G. Sinai, Ann. Math. **151**, 877 (2000).

[29] J. Bec and K. Khanin, Phys. Rep. **447**, 1 (2007).

[30] R. E. Bellman, *Dynamic Programming* (Dover, New York, 2003).

[31] G. K. Zipf, *Human Behavior and the Principle of Least Effort* (Addisson-Wesley Press, Cambridge, MA, 1949).

[32] A. Dabrowska *et al.*, Acta Phys. Pol. B **35**, 2109 (2004); Y. G. Ma *et al.* NIMROD Collaboration, Phys. Rev. C **71**, 054606 (2005).

[33] X. Campi and H. Krivine, Phys. Rev. C **72**, 057602 (2005).

[34] Note that for the diffusion-limited deposition of a hard-core lattice gas on a zero-temperature boundary a slower decay of the number density of clusters has been found, $c(h) \sim h^{-1/2}$ [27].